A geological and geochemical study of a sedimentary-hosted turquoise deposit at the Iron Mask mine, Orogrande, New Mexico

Josh C. Crook and Virgil W. Lueth

2014, pp. 227-233. https://doi.org/10.56577/FFC-65.227
Supplemental data: https://nmgs.nmt.edu/repository/index.cfml?rid=2014004

in:

Geology of the Sacramento Mountains Region, Rawling, Geoffrey; McLemore, Virginia T.; Timmons, Stacy; Dunbar, Nelia; [eds.], New Mexico Geological Society 65 th Annual Fall Field Conference Guidebook, 318 p.
https://doi.org/10.56577/FFC-65

This page is intentionally left blank to maintain order of facing pages.

A GEOLOGICAL AND GEOCHEMICAL STUDY OF A SEDIMENTARY-HOSTED TURQUOISE DEPOSIT AT THE IRON MASK MINE, OROGRANDE, NEW MEXICO

JOSH C. CROOK[1]* AND VIRGIL W. LUETH[2]

[1] Department of Earth & Environmental Sciences, New Mexico Institute of Mining and Technology, Socorro, NM (*deceased)

[2] New Mexico Bureau of Geology & Mineral Resources, New Mexico Institute of Mining and Technology, Socorro, NM, vwlueth@nmt.edu

ABSTRACT—Turquoise occurs in veins up to 8 cm thick in a shale unit of the Pennsylvanian Gobbler Formation at the Iron Mask claim in the Orogrande mining district, Otero County, New Mexico. Previous investigators have proposed three models for turquoise genesis: hydrothermal (magmatic-related), contact metasomatic, and supergene (weathering-related). The geologic setting and mineral assemblages at the Iron Mask claim suggest a supergene origin of turquoise. The presence of other oxidized copper minerals with turquoise supports the inference of Cu^{+2} mobilization derived from widespread porphyry-type copper mineralization in the district and subsequent introduction into the host shale. The ubiquitous presence of gypsum, which commonly occurs with turquoise, indicates that sulfuric acid solutions were abundant. X-ray fluorescence analysis of the shale indicates it is enriched in phosphate (up to 3 times average), which consists of apatite with minor xenotime. Dissolution textures exhibited by these minerals and depletion of phosphate in altered portions of the shale suggest they are the primary source of phosphate for turquoise genesis. Alteration within the shale units is confined to faults, fractures and along particular bedding planes, and characterized by the development of kaolinite, a feature characteristic of sulfuric acid-induced alteration. Coexisting supergene alunite and jarosite are found within the turquoise, indicating that the minerals precipitated from acid solutions at or near the surface of the phreatic zone. The presence of goethite in the mineral assemblage also indicates the solutions were cold, less than 100°C.

INTRODUCTION

The Orogrande district in the Jarilla Mountains, Otero County, New Mexico (Fig. 1) contains a number of turquoise deposits in a variety of host rocks. The majority are hosted by veins and veinlets in granitic or volcanic rocks, typical of most turquoise occurrences worldwide. The turquoise occurrence on the Iron Mask claim is somewhat unusual because it is hosted in shale and quartzite of the Pennsylvanian Gobbler Formation. The presence of turquoise in distinctly different host rocks in the Orogrande district provides a unique avenue to evaluate the potential origins of turquoise formation.

Turquoise, a semi-precious mineral often used in jewelry, has the chemical formula $Cu^{+2}Al_6(PO_4)_4(OH)_8 \cdot 4H_2O$ (Fleischer and Mandarino, 1991). Turquoise deposits are usually found in localized veins of altered and weathered aluminous granitic rocks (Palache et al., 1951). This mineral is abundant in New Mexico where it has been mined since ancient times; most famously at Cerrillos, the Burro Mountains, Santa Rita, and Orogrande (Pogue, 1915; Weber, 1979). Significant production of turquoise from mines in the Orogrande district was accomplished around Brice and most notably from the DeMueles (Providence) mine (Fig. 1).

Pogue (1915) described three settings in which turquoise occurs. These settings were determined by studying hundreds of worldwide turquoise occurrences and accounting for the sources of the various elements found in the mineral. Type I is a setting in which turquoise occurs in highly altered or weathered acid igneous rocks rich in feldspar. Type II occurs in sedimentary or metamorphic rocks near contacts with igneous rocks. Type III occurs in a non-igneous matrix, such as a sandstone or

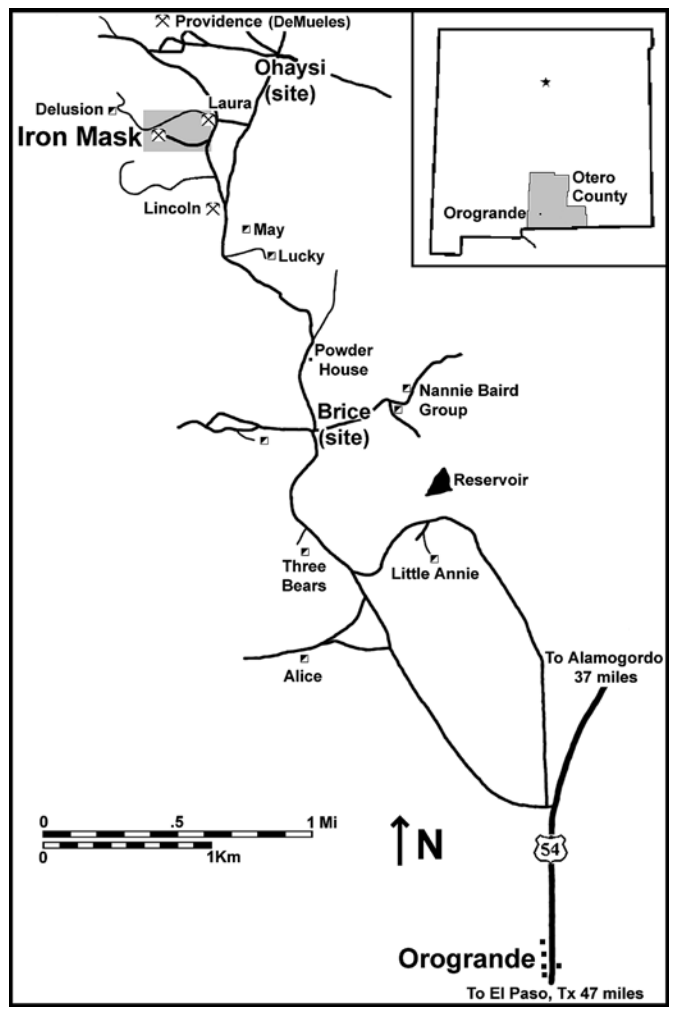

FIGURE 1. Location of the district (inset) and the Iron Mask claim (SW ¼ Sec. 3, T22S, R8E) within the Orogrande mining district. The shaded area at the Iron Mask is the area covered by the geologic map in Figure 2.

Supplemental data can be found at:
http://nmgs.nmt.edu/repository/index.cfm?rid=2014004

shale that has no genetic association with any igneous body. Less common settings exist including small turquoise crystals that occur in schist.

Pogue (1915) also offered three hypotheses on the origin of turquoise. The first was that turquoise formed from ascending solutions of magmatic origin in which the elements contained came from magma. This mode applied to occurrences of turquoise found in pegmatites. The second called for formation through the process of alteration of country rock by magmatic fluids. This would involve the formation of turquoise during hydrothermal alteration. The third hypothesis was that turquoise formed through the process of alteration and leaching of country rock by cold solutions during the course of weathering. Today, these modes of formation are referred to as hydrothermal, metasomatic, and supergene, respectively. These were proposed at a time when little had been written on turquoise and before most modern models of ore genesis were developed. Few papers of significance have discussed turquoise genesis since the Pogue (1915) monograph was published.

Turquoise occurrences are generally confined to the zone of oxidized minerals (Paige, 1912; Chavez, 2000). Unfortunately, the behavior of turquoise and other phosphate minerals in the weathering zone is not well understood. Most workers (Paige, 1912; Palache et al., 1951: North, 1982; Lueth, 1998; Chavez, 2000; Othmane et al., 2013) suggest that most turquoise forms through supergene processes.

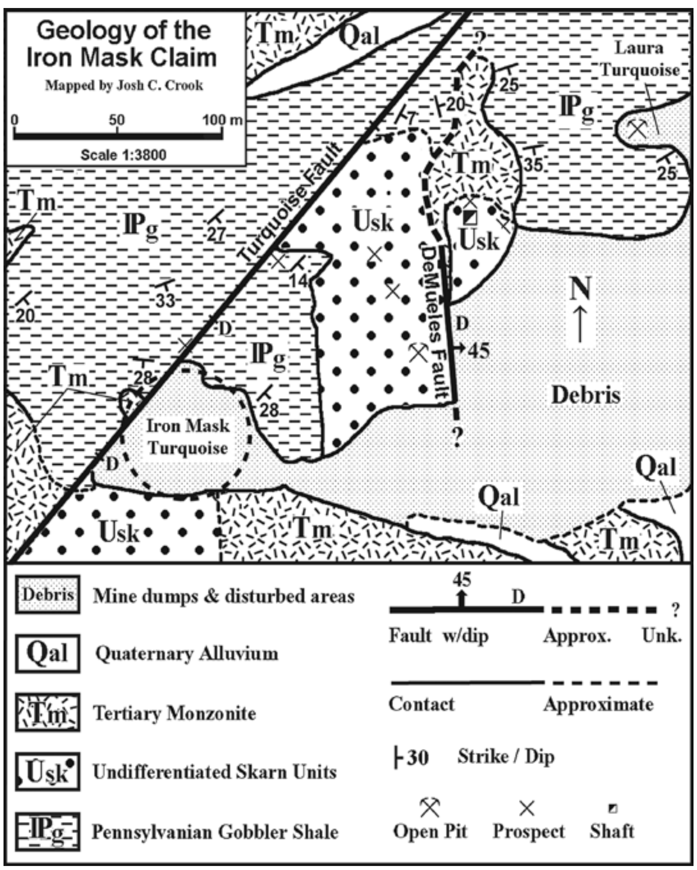

FIGURE 2. Geologic map of the Iron Mask and Laura claims (SW ¼ Sec. 3, T22S, R8E). Mapped by Josh C. Crook, March 7, 2002. The approximate area of the open pit developed by turquoise mine operations is indicated by the dashed line circle.

The most prominent geologic studies of the Orogrande area were made by Seager (1961), Schmidt and Craddock (1964), Beane et al. (1975), Bloom (1975), Strachan (1976), and North (1982). Kelley (1949) described the iron mines of the district. Bear Creek Mining Company's exploration program is reported in Andrews et al. (1976). Lueth (1998) described two turquoise deposits in the Orogrande district and began preliminary work on their origin.

GEOLOGY OF THE IRON MASK CLAIM

A geologic map covering the Iron Mask claim and adjacent Laura claim to the east was produced detailing surface exposures (Fig. 2) to better constrain the geologic features of the study area. The sedimentary units in the turquoise mine belong to the Pennsylvanian Gobbler Formation (Strachan, 1976; North, 1982). Schmidt and Craddock (1964) mapped these areas as undifferentiated metamorphic rocks. Bloom (1975) mapped them as Permian Panther Seep Formation, although the unit is not exposed in this part of the range (F. Kottlowski, personal commun., 1999). Although primarily composed of limestone, the Gobbler section exposed in the mine area is largely comprised of shale and quartzite.

The Gobbler shale has a "layered" appearance with alternating light and dark beds (Fig. 3). In fresh, unaltered samples, lighter-colored beds appear yellow to light gray and are typically coarser grained. Dark-colored beds appear dark gray to black and are predominantly clay. In altered samples, these layers appeared white and gray, respectively. Cross cutting fractures commonly display a light colored alteration selvage (Fig. 3) similar in color to the lighter colored layers. Some samples are coated with an alteration that appears rusty red-yellow suggesting the units may have contained authigenic pyrite. Grain sizes observed in shale are mostly clay with locally interbedded silt and sand layers that

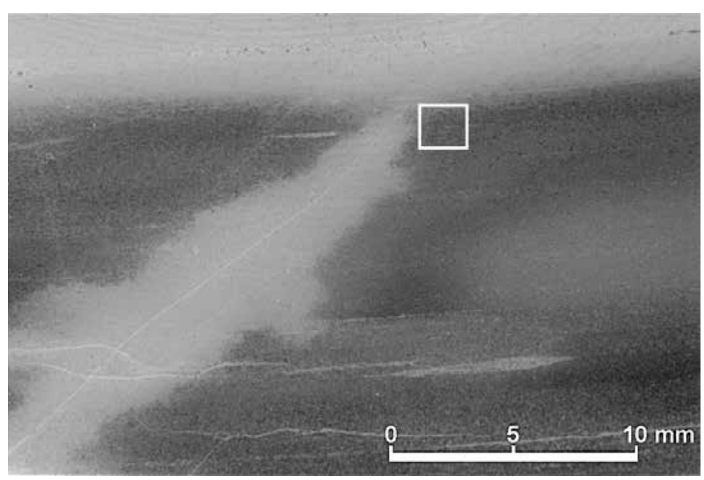

FIGURE 3. Thin section slide of the Gobbler shale. View is parallel to bedding. Note the light and dark colored beds and the alteration selvage surrounding the vein. The small veins are filled with gypsum. Square represents approximate area of back scatter electron image shown in Fig. 7.

display reverse-graded bedding. Mineralogically, the grains are composed primarily of clays (predominantly illite as determined by x-ray diffraction) and quartz. The coarsest layers consist of mostly angular grains of quartz.

A stratigraphic correlation was attempted between the turquoise-mineralized section at the Iron Mask claim with previously mapped shale units 1.6 km to the southeast. Strata from the Iron Mask turquoise pit were compared with strata in Strachan's "NB-1" through "NB-4" ('Nannie Baird') stratigraphic sections (Strachan, 1976). Shale from the turquoise pit appears to correlate with shale found in the "NB-4" section based on stratigraphic position and lithology. This would place the shale of the turquoise pit in the lower portion of the Gobbler Formation.

A Tertiary-age monzonite porphyry intrusive is exposed in the study area (McLemore et al., this guidebook). Schmidt and Craddock (1964) noted a large degree of textural variation within this rock type. The rock is predominantly comprised of fine-grained potassium feldspar – quartz matrix with phenocrysts of plagioclase and occasional quartz "eyes." A weak argillic alteration is pervasive in the immediate study area and varies significantly with intensity throughout the Jarilla Mountains. Sulfides occur scattered in the unit in various degrees of concentration. Where the monzonite contacts limestone-rich units, skarn mineralization is present. These skarns are predominantly comprised of andradite garnet, quartz, calcite, and magnetite-hematite. Shale-rich units are typically altered to limited zones of pyroxene hornfels along intrusive contacts. The contact metamorphic units were mapped as undifferentiated skarn unit for this study (Fig. 2).

Two faults were mapped in the study area (Fig. 2); a north trending fault (referred to as the DeMueles fault) and a northeast trending fault (referred to as the Turquoise fault). Both appear to be high-angle normal faults. The DeMueles fault strikes 355° and dips 45°E, and is located near the middle of the Iron Mask claim. Monzonite occurs on the west side of this fault, and skarn mineralization occurs on the east side. A marker bed of coarse quartz fragments in shale indicates that the east side of this fault is down-dropped. The Turquoise fault crosscuts the turquoise pit, strikes 45° and has a 90° dip. Drag folding, observed along the hanging wall in a prospect pit northeast of the turquoise pit, indicates that the southeast side of the Turquoise fault is down-dropped. The relationship between the Turquoise and DeMueles faults is ambiguous but the Turquoise fault appears to truncate the trend of the DuMueles fault. Displacement of the skarn and intrusive units across these two faults clearly indicates the faulting occurred after the emplacement of the intrusive units and skarn formation.

Turquoise mineralization in the turquoise pit is closely associated with altered host rocks. These rocks are leached so intensely in some areas that they appear white and are rich in clay minerals (predominantly kaolinite as determined by x-ray diffraction) and gypsum. The degree of clay-gypsum alteration in the turquoise pit is widely variable. Turquoise mining appears to have followed the most intense alteration along the Turquoise fault as the less altered shale appears darker and contains no turquoise. Alteration decreases toward the southwest end of the pit. The monzonite dike exposures in the pit contain only a few turquoise veinlets.

MINERALOGY OF THE TURQUOISE OCCURRENCE

Turquoise is found as nuggets and veinlets in fractures of every orientation. It tends to be chalky and occurs most commonly with gypsum, sericite, and kaolinite. Turquoise is occasionally observed as inclusions within plates of selenite (Fig. 4). Coexisting jarosite and alunite is also found with turquoise within portions of the Turquoise fault along with pyrite. Chalcosiderite was noted and it occurred less commonly with turquoise. Atacamite and malachite were observed as coatings on fractures. Malachite associated with minor azurite occurred as both coatings and in veinlets within the shale. Apatite and xenotime were identified during microprobe analysis of the shale. The exact species of apatite (chlor-, fluor-, or hydroxylapatite) was not determined. The occurrence of alunite, atacamite, chalcosiderite, and xenotime represent new records for the Orogrande mining district. All minerals reported were verified via x-ray diffraction (XRD) analysis at the New Mexico Bureau of Geology and Mineral Resources and scans are available in the supplementary data.

GEOCHEMISTRY

Two sampling patterns were devised to test the relative mobility of one turquoise component element, phosphorus, with respect to mineralization and alteration patterns. Copper and aluminum are widespread in the district and the distribution and abundance of those elements is too great to provide meaningful information. Phosphorus is much more limited in occurrence (predominantly as apatite) and abundance. Samples were analyzed for major element oxides using x-ray fluorescence. Select samples were also analyzed by electron microprobe. All x-ray fluorescence (XRF) spectroscopic and electron microprobe analyses (EMA)

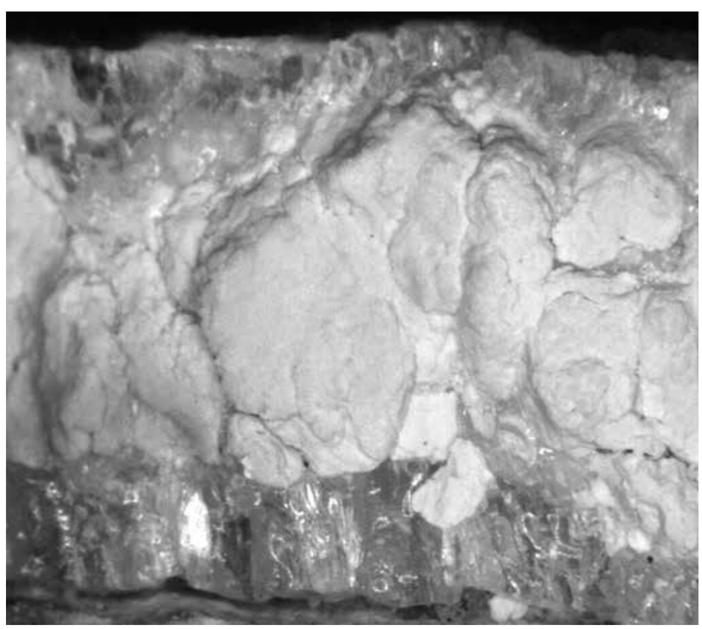

FIGURE 4. Nodular turquoise in the center of a vein surrounded by selenite gypsum. Thickness of the vein is 1.5 cm.

TABLE 1. Results of x-ray fluorescence analyses. * Denotes replicate sample, § Denotes phosphate standard, [1] Denotes vertical pattern sample, and [2] Denotes horizontal transect sample

Sample Number	SiO_2 wt.%	TiO_2 wt.%	Al_2O_3 wt.%	Fe_2O_3 wt.%	MnO wt.%	MgO wt.%	CaO wt.%	K_2O wt.%	Na_2O wt.%	P_2O5 wt.%	LOI wt.%	Total wt.%
990930-18A (lt) §	58.03	1.45	23.26	2.97	0.03	1.07	0.86	5.67	3.18	0.22	2.94	99.68
990930-18B (dk) §	57.46	1.38	23.00	1.56	ND	1.23	2.42	1.92	6.87	0.39	2.99	99.22
010500-10 [1]	64.90	1.27	20.45	0.67	ND	0.13	0.37	0.90	8.63	0.04	2.24	99.59
010500-12L [1]	59.84	1.63	23.70	0.62	ND	0.49	0.91	2.74	5.55	0.08	4.07	99.64
010500-12U [1]	59.51	1.57	23.33	0.81	ND	0.46	2.04	2.15	5.61	0.14	3.82	99.44
010500-13L [1]	59.66	1.58	23.57	0.55	ND	0.63	0.55	3.34	5.46	0.10	4.23	99.67
010500-13U [1]	61.33	1.46	23.02	0.56	ND	0.45	0.57	2.48	6.72	0.06	3.55	100.20
010500-13U *	61.00	1.45	23.00	0.56	ND	0.46	0.57	2.32	6.63	0.05	3.55	99.59
010500-14L [1] & [2]	60.24	1.53	23.74	0.77	ND	0.55	0.38	3.14	5.19	0.12	4.54	100.20
010500-14U [1]	64.77	1.28	20.08	0.70	ND	0.44	0.43	2.03	5.76	0.06	3.90	99.45
010500-17 [2]	55.20	1.91	27.01	0.60	ND	0.53	0.46	2.72	2.47	0.21	8.70	99.81
010500-18 [2]	58.61	1.71	24.39	0.51	ND	0.58	0.49	2.99	4.67	0.14	5.69	99.78
010500-19 [2]	58.30	1.73	24.17	0.58	ND	0.77	0.78	3.44	4.14	0.14	5.37	99.42
010500-19 *	58.25	1.73	24.15	0.59	ND	0.76	0.78	3.46	4.14	0.14	5.37	99.37
010500-20 [2]	60.86	1.50	23.28	0.55	ND	0.82	0.43	3.83	4.04	0.08	4.38	99.77

were performed in New Mexico Bureau of Geology and Mineral Resources laboratories using standard techniques described in the supplemental data. The results of these phosphorus analyses are presented in Table 1.

To determine the local background for phosphorus in the Gobbler Formation, away from any evidence of mineralization, one sample (990930–18) was collected from the southwest end of the turquoise pit where the shale appears least altered. The light and dark fractions (beds) of the relatively unaltered sample were analyzed separately. The light-colored fraction (sample 990930–18A) contained 0.22 ±0.01 wt. % P_2O_5, and the dark-colored fraction (sample 990930–18B) contained 0.39 ±0.01 wt.% P_2O_5. According to Rose et al. (1979), the average worldwide concentration of phosphorus in shale is 700 ppm (0.07 wt.%) which translates to approximately 0.16 wt.% P_2O_5. The shale of the turquoise pit appears to contain a greater than average concentrations of phosphate with values up to twice average shale (Table 1).

Samples were collected from a 15 cm vertical continuous rock column between two large (5 to 8 cm wide) turquoise-rich veins that trended parallel to bedding with two smaller veins in between (Fig. 5). A horizontal sample transect was collected between a large, mineralized vertical vein and more intensely-altered rocks located closer to the Turquoise fault (Fig. 6). Representative analyses for phosphorus along the traverses are also presented in both figures and provided in Table 1. From these diagrams, it is readily apparent that phosphorus has not been enriched significantly adjacent to veins and bedding associated with alteration. Phosphorus analyses of the host rocks adjacent to turquoise mineralization are actually depleted compared to the samples taken for background value determinations.

DISCUSSION

The unique character of the host rocks at the Iron Mask mine, the geological relationships within the deposit, and the observed mineralogy of the mineralization suggest that the origin of this deposit is unrelated to magmatic emplacement processes (Type I of Pogue, 1915). The majority of the turquoise mineralization is associated with the late stage faults noted in the mine area. The distribution of the mineral is highly influenced by structural control of the faults and specifically confined to the fractures developed on the hanging wall side. In all cases, the turquoise mineralization strongly follows fractures or bedding planes. These late faults all are most likely related to Basin and Range extension and not to the emplacement of the intrusive rocks in the area. The lack of hornfels development in the shale immediately adjacent to the monzonite, but separated by the Turquoise fault, confirms this relationship in the mine area. Accordingly, we interpret turquoise mineralization to postdate the age of porphyry copper deposit emplacement ca. 40 Ma (McLemore et al., this guidebook).

Orogrande turquoise could only have formed by hydrothermal alteration processes or by supergene mineralization processes, Types II or III of Pogue (1915). The distribution of turquoise in the Iron Mask study area is confined to the Gobbler Formation and no turquoise was noted in the skarn units that form specifically by metasomatic processes. Only minor occurrences were found in the monzonite intrusive, where they are confined to fractures in proximity to the main faults and associated with weathering derived minerals, specifically goethite, gypsum and/or jarosite. Turquoise mineralization occurs irrespective of the degree of hydrothermal alteration within the monzonite, a feature

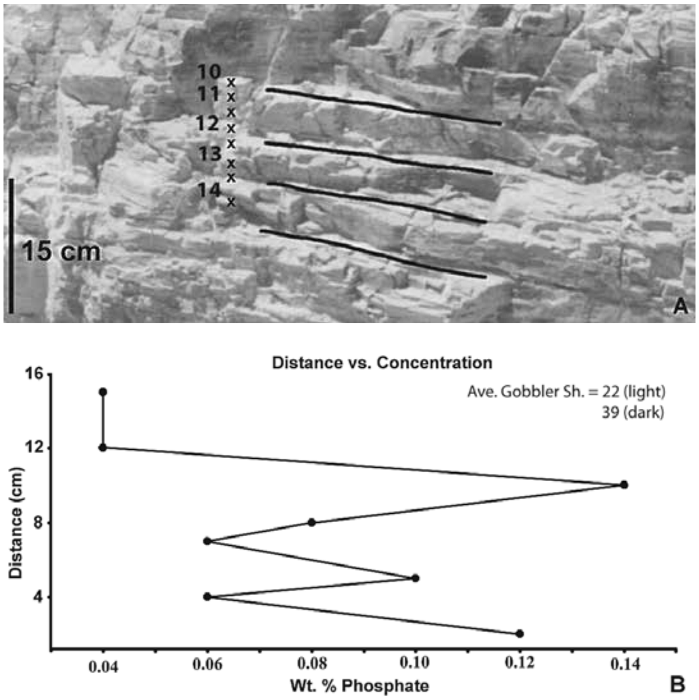

FIGURE 5. Vertical sample pattern. A. Photo of the pattern; the view is looking northwest toward the high-wall; x represents exact sample location; horizontal lines show the location of turquoise veins parallel to bedding. Numbers represent last two values of sample number from Table 1. Samples 12–14 consist of upper (U) and lower (L) pairs as presented in Table 1. B. Graph of the distance versus phosphate concentration. Average background P concentrations (wt.%) in light and dark layers are noted on the graph.

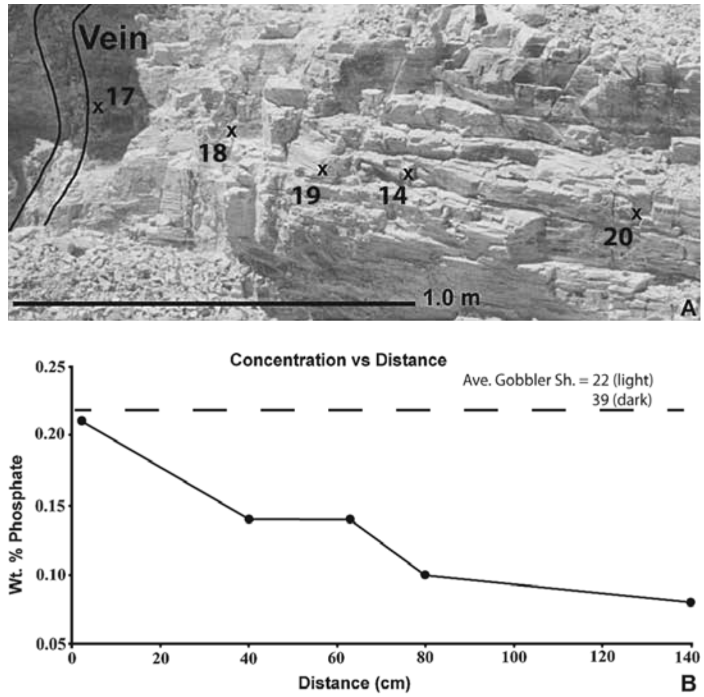

FIGURE 6. Horizontal sample pattern. A. Photo of the pattern; the view is looking northwest toward the high-wall; x represents exact sample location. Numbers represent last two values of sample number from Table 1. B. Graph of phosphate concentration versus distance. Average background P concentrations (wt.%) in light and dark layers are noted on the graph and the dashed line represents 0.22 wt.% P. The area labeled "vein" is coincident with the trace of the Turquoise fault.

noted at the other turquoise deposits in the district. Alteration of the host shales and silts is not pervasive and is mainly confined to fractures. It was only noted in coarser grained beds adjacent to late stage faults. Alteration selvages are common along fractures and faults indicating focused fluid flow by infiltration along major faults. Formation of turquoise by metasomatic processes (Type II) appears less feasible than mineralization induced by supergene weathering (Type III).

Porphyry style copper mineralization that consists of disseminated pyrite and chalcophyrite has long been recognized in the Orogrande district (Beane et al., 1975). Pyrite and chalcopyrite in the presence of water and oxygen produces sulfuric acid, iron oxide compounds and Cu^{+2} (Anderson, 1982). The acidic solution provides a media for chemical reactions, and a transport mechanism into and out of the wall rock. Papers by Anderson (1982), Alpers and Brimhall (1989), and Chavez, (2000) discuss the process of pyrite oxidation under various chemical and environmental conditions and its subsequent mineralogy. Four moles of acid are generated from the oxidation of each mole of pyrite (Alpers and Brimhall, 1989). Ferric sulfate is formed if abundant pyrite is available (Chavez, 2000). Goodell and Lueth (1998) reported the ferric sulfate minerals copiapite immediately northwest of the study area, and presence of jarosite "spider webbing" the turquoise indicates high oxygen activity. Secondary gypsum is widespread throughout the study area indicating that sulfide oxidation and generation of abundant sulfuric acid was extensive since no gypsum bearing units are present in the Jarilla Mountains. Gypsum is a reaction product of sulfuric acid and calcium-rich rocks or minerals that forms at low temperatures (Freyer and Voight, 2003). Gypsum is often observed encasing turquoise in veins located in the fault zones (Fig 4). The presence of multiple copper oxide phases indicates an abundance of mobilized copper (Chavez, 2000). Cu^{+2} is mobile in oxidizing environments where solutions have a pH below 3.5 (Anderson, 1982). The presence of oxidized copper minerals, atacamite, azurite, malachite and chrysocolla confirms the availability of copper in the weathering solutions.

At the low pH and high oxygen activities that mobilize copper, phosphorus is similarly mobilized as PO_4^{-3} (Magalhães et al., 1986). The patterns of phosphorus concentrations in the host shale, determined by XRF, suggest that phosphate was leached from the wall rocks in the mine area and mobilized with acidic solutions that flowed through fractures. XRF data from the vertical sampling pattern suggest that the shale was once phosphate-rich, but it was leached from the host rock into the veins. Phosphate concentrations ranged from 0.04% ±0.01% P_2O_5 closest to veins and in altered selvages and increased to 0.14% ±0.01% P_2O_5 away from veins and selvages. Figure 5 summarizes the results of the vertical sampling pattern. Data from the horizontal sampling pattern

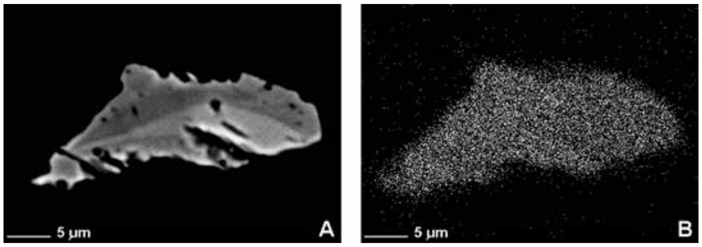

FIGURE 7. Xenotime grain in partially altered shale that was located in the white box in Figure 3, sample 010500–18. A. Backscatter electron image; light areas represent a higher atomic mass (Z). Notice the embayments on the margins of the grains due to dissolution. B. Phosphorus map with white dots and light areas that represent phosphorus, contained in the xenotime.

(Fig. 6) indicate that more intense leaching of phosphate occurred in the vicinity of the Turquoise fault. Rocks nearest to this fault are nearly white and are comprised of kaolinite-smectite-gypsum. Illite, common in unaltered shale, is lacking suggesting significant effects of hydrolysis in the altered shales. The concentrations ranged from 0.21% ±0.01% P_2O_5 nearest the fault, but not in the turquoise-gypsum vein to 0.08% ±0.01% P_2O_5 farthest from the fault.

In conjunction with the XRD data, microprobe image analyses also suggests that phosphate from the shale was leached (Fig. 7). Apatite and xenotime grains in altered shale units display evidence of dissolution on their margins as embayments. Similar textures were absent in the apatites and xenotimes taken farthest from alteration.

Likewise, the monzonite in the study area could have provide the phosphate under similar conditions by the leaching of apatite that is present in these units as noted by Schmidt and Craddock (1964; Plate 2). However, the monzonite units in the mine area are stratigraphically, topgraphically, and hydrologically (assuming downward fluid flow) below the turquoise mineralization. In contrast, at other turquoise deposits in the district, hosted by the granitic rocks, a source of phosphate from the granitic host rocks is probable if the same supergene processes were in operation at those deposits, which is suggested by the similar mineralogy of the vein turquoise deposits across the district.

Turquoise in the Iron Mask deposit is invariably mixed with other minerals, specifically, goethite, pyrite, gypsum, jarosite, alunite, quartz and kaolinite. In all cases the goethite, alunite, and jarosite minerals tend to be fine grained, anhedral mixtures. Not all associated phases are always found in a single sample, but specific assemblages are present that help to constrain the geochemical environment of formation. Perhaps the most important assemblage noted in the turquoise consists of jarosite-pyrite-alunite-goethite. The presence of all four minerals can be used to determine the pH and Eh (Fig. 8) of the mineralizing waters at around 1.8 to 2.5 and 0.5 respectively in waters at standard temperature and pressure (Keith et al., 1979; Lueth et al.,1998). These values are typical for waters in contact with oxidizing sulfide minerals. The presence of goethite and lack of hematite in the assemblage precludes formation at temperatures over 100°C

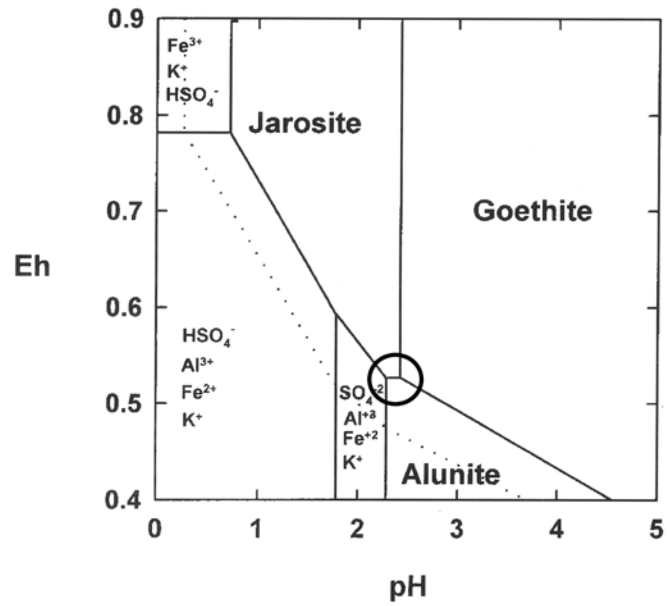

FIGURE 8. Eh-pH diagram depicting the stability fields of goethite-jarosite-alunite and aqueous species at 25° C and 101.3 kPa. Activities of species used in the calculations are: $(a_{\Sigma S}) = 10^{-2}$ m; $(a_{\Sigma Fe^{2+},Fe^{3+}}) = 10^{-1}$ m; $(a_{Al^{3+}}) = 10^{-3}$ m; $(a_{K^+}) = 10^{-3}$ m. Dashed lines represent $(a_{\Sigma Fe^{2+},Fe^{3+}}) = 10^{-3}$. Diagram modified from Lueth et al., 1998 using data of Keith et al., 1979. The circle represents the Eh-pH conditions of turquoise formation at the Iron Mask mine.

(Stoffregen, 1993). The lack of significant crystal size and perfection in the alunite/jarosite also suggests a low temperature of formation supporting a supergene origin (Lueth, 2006).

The phreatic zone in supergene environments is important for the formation of copper enrichment blankets (Chavez, 2000). Neutralizing reactions with the wall rock, especially those that are rich in feldspars, micas, and limestone control the pH of the solution and precipitate supergene minerals. Supergene alunite and jarosite were found in a turquoise vein along the Turquoise fault. The geochemical boundary between the formation of supergene jarosite and alunite is at the surface of the phreatic zone (Rye et al., 2000). Jarosite, stable at lower pH and higher oxygen fugacity, is commonly limited to the vadose zone, whereas alunite forms at or below the surface of the phreatic zone. The occurrence of supergene alunite and jarosite with turquoise indicate that turquoise precipitated in solution conduits at or near the surface of the phreatic zone as neutralizing reactions took place. Both these minerals can be dated and suggest the potential for dating the position of water tables during the natural destruction of porphyry copper deposits. By proxy, turquoise may be an indicator mineral of water table position at the time of supergene mineralization.

CONCLUSIONS

The geological, mineralogical and geochemical information derived from this study suggests the formation of the turquoise at the Iron Mask mine appears to be the product of supergene mineralization processes, not associated with hypogene processes. Porphyry copper mineralization consisting of disseminated pyrite and chalcopyrite oxidized and generated large quantities of sulfuric acid and copper ions in solution. These acidic solutions moved along pre-existing faults and fractures and interacted with shales of the Gobbler Formation. The acid solutions leached phosphate from apatite and xenotime, which are found in the host shale. Local rocks are aluminum-rich and at low pH could also have provided the necessary dissolved oxidized aluminum. Turquoise and associated minerals precipitated where these solutions were neutralized near the surface of the phreatic zone.

ACKNOWLEDGMENTS

The authors wish to acknowledge several organizations and individuals who made this possible. An undergraduate research grant from the New Mexico Geological Society to JCC paid for most of the research expenses. The New Mexico Bureau of Geology and Mineralogical Resources provided the X-ray and electron microprobe facilities and laboratories to carry out this research. Several other staff members of the New Mexico Bureau of Geology and Mineral Resources were very helpful including, Chris McKee, Dr. Nelia Dunbar, Robert W. Eveleth, and Dr. Frank E. Kottlowski. Dr. Nigel Blamey of the New Mexico Institute of Mining and Technology reviewed an early manuscript of this research. Ryan L. Robinson assisted with the field work. The authors are also grateful for the insight and comments of Robert M. North of the Phelps Dodge Chino Mines Company who reviewed an earlier version of this paper and Drs. Virginia McLemore and Andrew Campbell who provided a final review of this manuscript.

REFERENCES

Alpers, C.N. and Brimhall, G.H., 1989, Paleohydrologic evolution and geochemical dynamics of cumulative supergene metal enrichment at La Escondida, Atacama Desert, Chile: Economic Geology, v. 84, p. 229–255.

Anderson, J.A., 1982, Characteristics of leached capping and techniques of appraisal, *in* Titley, S.R., ed. Advances in geology of the porphyry copper deposits southwestern North America: Tucson, University of Arizona Press, p. 275–295.

Andrews, R.K., Lyons, J.I., and Martineau, M.P., 1976, Report and recommendations, Orogrande appraisal, geologic work and drilling program: unpublished report to Bear Creek Mining Company, Tucson Office, 33 p.

Beane, R.E., Jaramillo, L., and Bloom, M.S., 1975, Geology and base metal mineralization of the southern Jarilla Mountains, Otero County, New Mexico: New Mexico Geological Society, Guidebook 26, p. 151–156.

Bloom, M.S., 1975, Mineral paragenesis and contact metamorphism in the Jarilla Mountains, Orogrande, New Mexico [MS Thesis]: Socorro, New Mexico Institute of Mining and Technology, 81 p.

Chavez, W.X., Jr., 2000, Supergene oxidation of copper deposits: zoning and distribution of copper oxide minerals: Society of Economic Geologists, Newsletter n. 41, p. 1, 10–21.

Fleischer, M. and Mandarino, J.A., 1991, Glossary of mineral species 1991: The Mineralogical Record, Inc., p. 205.

Freyer, D., and Voight, W., 2003, Crystallization and phase stability of $CaSO_4$ and $CaSO_4$-based salts: Monatschefte fur Chemie, v. 134, p. 693–719.

Goodell, P.C., and Lueth, V.W., 1998, Geology and mineralogy of the Jarilla (Orogrande) mining district, New Mexico (abs.): New Mexico Geology v. 17, n. 1, p. 14–15.

Keith, W.J., Calk, L., and Ashley, R.P., 1979, Crystals of coexisting alunite and jarosite, Goldfield, Nevada: U.S. Geological Survey, Professional Paper 1124-C, p. C1–C5.

Kelley, V.C., 1949, Geology and economics of New Mexico iron-ore deposits: University of New Mexico, Publication in Geology no. 2, p. 181–193.

Lueth, V.W, 1998, Two diverse origins for turquoise at the Orogrande mining district, Otero County, New Mexico (abs.): New Mexico Geology v. 20, n. 2, p. 65.

Lueth, V.W. Goodell, P. C., Heizler, M.T. and Peters, L., 1998, Geochemistry, geochronology, and tectonic implications of jarosite mineralization in the northern Franklin Mountains, Doña County, New Mexico: New Mexico Geological Society, Guidebook 49, p. 309–316.

Lueth, V.W., 2006, Textural and stable isotope discrimination of hypogene and supergene jarosite and environment of formation effects on $^{40}Ar/^{39}Ar$ geochronology (abs.): Workshop on Martian Sulfates as Recorders of Atmospheric-Fluid-Rock Interactions, Lunar and Planetary Institute Contribution 1331, p. 51.

Magalhães, M.C.F., de Jesus, J.P., and Williams, P.A., 1986, Stability constants and formation of Cu(II) and Zn(II) phosphate minerals in the oxidized zone of base metal orebodies: Mineralogical Magazine v. 50, p. 33–39.

McLemore, V.T., Dunbar, N., Heizler, L., and Heizler. M., 2014, Geology and mineral deposits of the Orogrande mining district, Jarilla Mountains, Otero County, New Mexico: New Mexico Geological Society, Guidebook 65.

North, R.M. 1982, Geology and ore deposits of the Orogrande mining district, Otero County, New Mexico: New Mexico Bureau of Mines and Mineral Resources Open File Report 370, 22 p.

Othmane, G., Hull, S., Fayek, M., Rouxel, O., Lahd Geagea, M., Kyser, T. K., Abdu, Y., Hawthrone, F. C., McEleney, K., and Freund, M., 2013, H and Cu variability and alteration in turquoise (abs.): Geological Society of America, Abstracts with Programs, v. 45, n. 7, p. 832.

Paige, S., 1912, The origin of turquoise in the Burro Mountains, New Mexico: Economic Geology, v. 7, p. 382–392.

Palache, C., Berman, H., and Frondel, C., 1951, The system of mineralogy: Volume II, 7th ed., London, John Wiley and Sons, p. 946–951.

Pogue, J.E., 1915, The turquoise: A study of its history, mineralogy, geology, ethnology, archaeology, mythology, folklore, and technology: National Academy of Science Memoir 12, 162 p.

Rose, A.W., Hawkes, H.E., and Webb, J.S., 1979, Geochemistry in mineral exploration: 2nd ed., Academic Press, London, p. 564.

Rye, R.O., Bethke, P.M., Lanphere, M.A., and Steven, T.A., 2000, Neogene geomorphic and climatic evolution of the central San Juan Mountains, CO: K/Ar age and stable isotope data on supergene alunite and jarosite from Creede mining district, *in* P.M. Bethke and R.L. Hay, eds., Ancient Lake Creede: its volcano-tectonic setting, history of sedimentation and relation to mineralization in the Creede mining district: Geological Society of America Special Paper 346, p. 95–103.

Schmidt, P.G. and C. Craddock, 1964, Geology of the Jarilla Mountains, Otero County, New Mexico: New Mexico Bureau of Mines and Mineral Resources Bulletin 82, 55 p.

Seager, W., 1961, Geology of the Jarilla Mountains, Tularosa Basin [MS Thesis]: Albuquerque, University of New Mexico, 80 p.

Stoffregen, R.E., 1993. Stability relations of jarosite to natrojarosite at 150–250°C: Geochim. Cosmochim. Acta, v. 57: p. 2417–2429.

Strachan, D.G., 1976, Stratigraphy of the Jarilla Mountains, Otero County, New Mexico [MS Thesis]: Socorro, New Mexico Institute of Mining and Technology, 134 p.

Weber, R.H., 1979, Turquoise in New Mexico: New Mexico Geology, v. 1, p. 39–40.